Smart Materials and Structures

PAPER

A robotic multiple-shape-memory ionic polymer–metal composite (IPMC) actuator: modeling approach

To cite this article: Qi Shen *et al* 2019 *Smart Mater. Struct.* **28** 015009

IOP Publishing Smart Materials and Structures
Smart Mater. Struct. **28** (2019) 015009 (11pp) https://doi.org/10.1088/1361-665X/aaeb83

A robotic multiple-shape-memory ionic polymer–metal composite (IPMC) actuator: modeling approach

Qi Shen[1], Tyler Stalbaum[1], Nazanin Minaian[1], Il-Kwon Oh[2] and Kwang J Kim[1]

[1] Department of Mechanical Engineering, University of Nevada, Las Vegas, Nevada, 89154, United States of America
[2] Mechanical Engineering Department, University of Nevada, Reno, Nevada, 89557, United States of America

E-mail: kwang.kim@unlv.edu

Received 2 August 2018, revised 19 October 2018
Accepted for publication 25 October 2018
Published 23 November 2018

Abstract
The multiple-shape-memory ionic polymer–metal composite (MSM-IPMC) actuator can demonstrate complex 3D deformation. The MSM-IPMC has two distinct characteristics, which are the electromechanical actuation effect and the thermal-mechanical shape memory effect. The bending, twisting, and oscillating motions of the actuator could be controlled simultaneously or separately by means of thermal-mechanical and electromechanical transduction. In this study, a theoretical model for the MSM-IPMC was developed and experimentally investigated. Based on previous studies on the electromechanical actuation effect of ionic polymer–metal composite (IPMC), a comprehensive physics-based model of MSM-IPMC which couples the actuation effect and the multiple shape memory effect was developed. To verify the model, an MSM-IPMC sample was prepared and used in experimental testing. The simulation results were shown to be in good agreement with the experimental results obtained. The multiple shape memory and recovery rate of three different polymers, namely the Nafion, Aquivion and GEFC of different ions, which are the hydrogen, lithium and sodium, were also tested. Based on the results, it is shown that all the polymers demonstrate the multiple shape memory effect with varying amounts of programmable shapes. The ion type was shown to have an influence on the broad glass transition range of the polymers, which in turn dictated the number of possible programmable shapes for each membrane. The current study is beneficial for the better understanding of the multiple shape memory effect of MSM-IPMC.

Keywords: complex 3D deformation, IPMC, shape memory

(Some figures may appear in colour only in the online journal)

1. Introduction

The ionic polymer–metal composite (IPMC) has been studied for decades due to its unique mechanoelectrical and electromechanical transduction mechanisms [1–8]. Such composites are commonly made with ionomer materials such as Nafion, Aquivion, or GEFC. Metal layers are chemically plated to both sides of a rectangular sheet of the ionomer. The samples are cut to size, and the edges are trimmed to create discrete electrodes. Chemically stable metals, such as gold and platinum, are usually used for this purpose [9]. Recently, palladium and graphene have also been used to plate the surface of the polymer [3, 10–12]. When a voltage is applied on both sides of the IPMC, the mobile ions inside the polymer migrate to the cathode and accumulate at the boundary of the polymer, causing the IPMC to bend [13]. Alternatively, if the IPMC is mechanically deformed, a detectable voltage is generated on the surface of IPMC. Many physical models have been developed to describe these transductions [2, 14–17]. Some interesting characteristics of IPMC materials include its inherent softness, resilience, and low operational power. Many scientists and engineers have developed robotic systems using IPMCs as sensors and actuators [18–23].

Recently, it was found that Nafion, which is the intermediate layer typically used in an IPMC, has multiple shape memory effects [24]. A hybrid actuator utilizing both the multiple shape memory phenomenon and the electromechanical transduction effects of IPMC actuators was developed by the authors [25]. The original shape of the sample is named S0. To program the first shape, the IPMC is formed into shape S1, heated to temperature T1, then cooled to a lower temperature T1′, such that $T1' < T1$. The programming process of S1 is then completed and is thusly 'memorized' within the range from T1′ to T1. The process can be repeated multiple times. Different shapes S2 and S3 can be programmed within the temperature ranges from T2′ to T2 and T3′ to T3, respectively. It should be noted that $T3' < T3 < T2' < T2 < T1' < T1$. As the polymer is reheated from T3′ to T1, the polymer recovers the programmed shapes from S3 to S0 within their corresponding temperature ranges. These shape recoveries are likely possible because of the broad glass transition ranges over the recovery temperatures. Nafion, with the ability to remember multiple shapes, has promising potential for applications in actuators, sensors and smart devices.

Based on the electromechanical transduction and multiple shape memory effect, the authors have introduced a hybrid soft-robotic actuator, the multiple-shape-memory ionic polymer–metal composite (MSM-IPMC) [25]. This actuator can perform deformations of multiple degrees of freedom by taking advantage of these effects.

The shape memory properties of Nafion have recently been studied. Xie reported that annealed dry Nafion samples can be programmed to memorize up to four different shapes [24]. Rossiter *et al* presented the shape memory properties of Nafion-based IPMCs [26]. The IPMC was programmed to specific shapes by applying deformation through external force and electrical actuation. There was an observable slow decay along with the shape memory effect. Xiao *et al* applied a quasi-static, nonlinear viscoelastic model using a discrete spectrum of relaxation times to model the shape memory effect of Nafion [27]. Xie proposed a physical theory to explain this behavior [28]. The critical point for this theory is that a single broad thermal transition can be regarded as the collective contribution of numerous infinitely sharp transitions continuously distributed in the broad temperature range. Previously the authors laid out a theoretical framework in terms of finite element based free-energy density to describe the shape memory effect of the IPMC [29].

While experimental tests on the shape memory properties of Nafion have been conducted, limited work has been done concerning the theoretical investigation of the multiple shape memory effect of Nafion. A model is desirable to quantify the thermo-mechanical transduction.

The first goal of this study is to develop a multiphysics model of the MSM-IPMC. A theoretical model of the multiple shape memory effect, based upon thermal stress analysis, was developed. It was assumed that the multiple shape memory effect is caused by induced internal thermal stress and memorized Young's moduli during the programming process. As the MSM-IPMC is reheated to each temperature, the corresponding thermal stress is applied on the MSM-IPMC, and Young's modulus is recovered, which results in the shape recovery of the MSM-IPMC. This model was coupled with the electrical actuation model of IPMCs, which was reported in the authors' previous work [13, 30]. The multiphysics model of the MSM-IPMC was obtained based on the coupled model. In-lab fabricated MSM-IPMC samples were experimentally tested. The Dynamic Mechanical Analyzer (DMA) was used to test the multiple shape memory effect. Electromechanical actuation and the multiple shape memory effect of the MSM-IPMC were demonstrated simultaneously. The simulation results and experimental results were compared. This work should provide keen insight into the underlying physics of multiple shape memory effects.

The second goal of this study is to characterize the multiple shape memory effect of the MSM-IPMC. Three different ionic exchange membranes, Nafion, Aquivion, and GEFC, with three different ions, Hydrogen (H^+), Lithium (Li^+), and Sodium (Na^+), were fabricated and used for testing. This makes a total of nine different combinations of membrane and cation type for the MSM-IPMC samples. The multiple shape recovery of the samples was qualitatively tested. A physical understanding based on enthalpy and free energy was proposed to describe the multiple shape memory performance of the different samples. This work can also be used to study the multiple shape memory effect of other shape memory polymers.

2. Mathematical model

2.1. Modeling of the multiple shape memory effect

Several works have been reported on the modeling of the shape memory behavior of Nafion. One theory is that the shape memory process can be directly modeled by considering the glass transition model [27]. A temperature-dependent relaxation time or viscosity was assumed in the model. During the glass transition, the relaxation time changes significantly. This allows the materials to store a temporary shape and recover a permanent shape.

In this study, the authors expand upon this model through segmenting the broad glass transition region into independent sections, as illustrated in figure 1. Through previous studies, it was found that Nafion has multiple shape-memory properties which can be programmed into several different shapes and controlled through thermal or electrical inputs. Rather than seeing the glass transition range as solely a broad region, it can be assumed that this region consists of a consecutive series of distributed glass transition ranges. The current accepted range of the broad glass transition temperature for Nafion ranges from 55 °C to 140 °C, where Nafion can be programmed with multiple unique shapes with recovery under

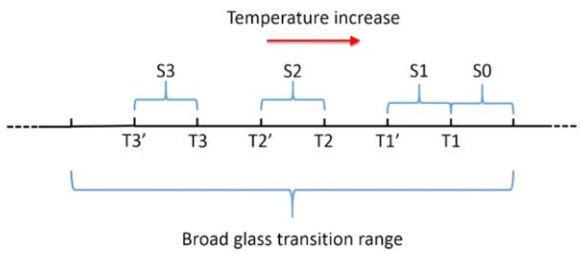

Figure 1. Illustration of the multiple shape memory effect. The memorized shapes are identified as S1 through S3, which correspond to the temperature ranges of T1 to T1′, T2 to T2′, and T3 to T3′. The original shape is identified as S0 [31].

varying temperatures. In this work, a theoretical model based on the above theory of segmented glass transition temperatures for the multiple shape memory effect has been coupled with the electromechanical model of the IPMC. This work assumes that the multiple shape memory effect is caused by an imposed internal stress with a specific Young's modulus 'memorized' during the programming process. As the MSM-IPMC is reheated to each temperature, the internal stress is released, and Young's modulus is recovered, which results in the shape recovery of the sample.

The internal stress, which is caused by the deformation of polymer chain at the glass transition temperature, is released on the MSM-IPMC during each shape recovering process. The expression of the internal stress can be expressed as [32]

$$\sigma(t) = \sum_i^N \frac{\rho_n RT(t)}{M_C}\left(\alpha_i - \frac{1}{\alpha_i^2}\right) \quad (1)$$

where i refers to each individual shape memory process, N is the total number of the shape memory process, $T(t)$ is the temperature, ρ_n is the density of the polymer, R is the gas constant, M_C is the molecule weight of the polymer and α_i is the extension ratio. L, W and $2h$ are the length, width and thickness of the MSM-IPMC sample, respectively. The α_i can be denoted as

$$\alpha_i = 1 + \varepsilon_i \quad (2)$$

where ε_i is the programmed strain of the polymer at each shape memory process. As the MSM-IPMC is reheated to a previously programmed temperature, the previously stored Young's modulus is applied accordingly. The Young's modulus can be expressed as

$$Y(t) = Y^{eq} + \sum_i^N Y_i^{neg} \exp\left(a\left(\frac{T(t)}{T_i} - 1\right)\right) \quad (3)$$

where Y^{eq} is the equilibrium Young's modulus, Y_i^{neg} is the nonequilibrium Young's modulus, a is the coefficient related with the shape memory process, T_i is the reference temperature corresponding to the programming temperature at each shape memory process. Using linear beam defection theory, the tip displacement w_s of the IPMC beam element relating to the longitudinal coordinate direction, z, can be denoted as

$$\frac{d^2 w_s(z, t)}{dz^2} = \frac{M(z, t)}{YI} \quad (4)$$

where I is the moment of inertia of the IPMC actuator and $I = 2/3Wh^3$. By relating the induced stress $\sigma(\pm h, z, t)$ to the bending moment, one can obtain

$$\sigma(\pm h, z, t) = \frac{\pm hM(z, t)}{I} \quad (5)$$

Combing equations (3)–(5), the tip displacement w_s induced by the multiple shape memory effect can be expressed as

$$w_s(L, t) = \frac{\sum_i^N \frac{\rho_n RT(t)}{M_c}\left(\alpha_e - \frac{1}{\alpha_e^2}\right)L^2}{2h\left(Y^{eq} + \sum_i^N Y_i^{neq} \exp\left(a\left(\frac{T(t)}{T_i} - 1\right)\right)\right)} \quad (6)$$

2.2. Modeling of the MSM-IPMC

This work extends upon previous developments from the authors which combines models for the resistance change effect of surface electrodes and the charge dynamics of the IPMC. The model utilized principles of metallic microstructure to describe the surface resistance change of the IPMC while simultaneously coupled with the Poisson-Nernst-Planck equations for describing the transport phenomenon and charge density within the polymer [13]. The system of equations is solved by finite element methods [13]. To summarize the work in brief, the deformation $w_a(L, s)$ caused by the actuation effect under the voltage $V(s)$ can be obtained by solving the following equation in the frequency domain as [13]

$$w_a(L, s) = \frac{\alpha L}{hY(t)} \frac{(-\exp(J(s)) + J(s) + 2)\left(1 + \frac{1}{J(s)}\right)}{J(s)K(s)} \times \sinh(A(s)h)V(s) \quad (7)$$

with

$$J(s) = -\frac{DW_e h_e R_e}{h} \times \frac{\left(\frac{2\sinh(A(s)h)}{A(s)} + 2h\cosh(A(s)h)\right)\left(\frac{A(s)}{F} - \frac{FC_0}{RT\hat{\varepsilon}A(s)}\right)}{K(s)}$$

$$K(s) = \frac{2\sinh(A(s)h)}{\hat{\varepsilon}A^2(s)} + 2h\cosh(A(s)h)\left(\frac{RTA(s)}{F^2C_0} - \frac{1}{\hat{\varepsilon}A(s)}\right)$$

$$A(s) = \sqrt{\frac{B+s}{D}}$$

$$B = \frac{\hat{z}\mu F^2 C_0}{\hat{\varepsilon}}$$

where α is the proportional coefficient that relates the charge density at the boundary of polymer to the induced stress [33], Y is the Young's modulus, s is the Laplace domain variable, D is the diffusion constant, F is the Faraday constant, C_0 is the constant anion concentration, R is the gas constant, $\hat{\varepsilon}$ is the

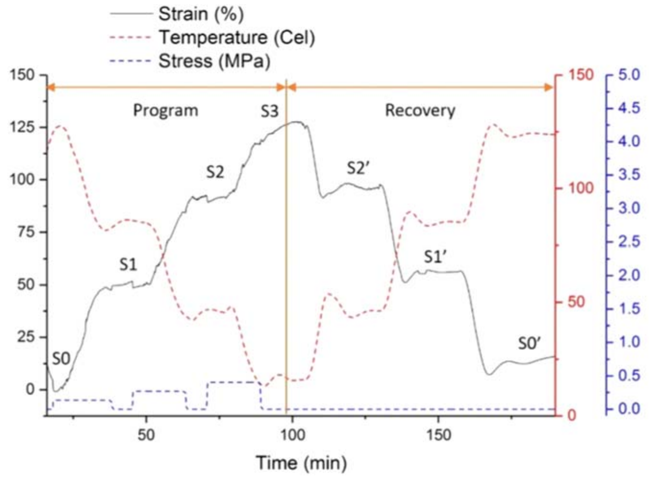

Figure 2. Quadruple shape memory properties of the MSM-IPMC. The programming takes place during t < 100 min, where the applied programming stress and temperature ranges are shown. The shape recovery is shown during t > 100 min [31].

absolute dielectric constant, W_e is the width of the surface electrode, h_e is the thickness of the surface electrode, $\hat{z}$ is the charge number, μ is the mobility of cations, R_e is the resistance of the surface electrode. The reader is referred to Ref. [13] for the derivation of equation (7).

By solving equation (7), the deformation $w_a(L, s)$ of the IPMC under the voltage can be obtained. MATLAB was used to obtain the numerical solution for $w_a(L, s)$. Then $w_a(L, s)$, which is in the frequency domain, was converted to the time domain $w_a(L, t)$.

Based on the $w_s(L, t)$ induced by the multiple shape memory effect and $w_a(L, t)$ induced by the actuation effect, the total tip displacement $w_t(L, t)$ of MSM-IPMC can be obtained as

$$w_t(L, t) = w_s(L, t) + w_a(L, t). \tag{8}$$

3. Experimental investigation

3.1. Multiple shape memory effect model validation

The multiple shape memory effect was tested by Dynamic Mechanical Analysis (DMA). An MSM-IPMC sample of 20 mm in length, 4.95 mm in width and 0.18 mm in thickness was used for the test. The selected sample dimensions were based on acceptable electromechanical performance. The ionic exchange membrane used was Nafion. Figure 2 shows the quadruple shape memory properties of the MSM-IPMC. The original shape of the sample was identified as S0. External stresses were applied to the sample under their respective programming temperature ranges. Three different shapes S1, S2 and S3 were programmed at the temperature range 130 to 85 °C, 85 to 55 °C and 55 to 20 °C, respectively, by applying uniaxial stress in the DMA. The deformation of the sample was measured in terms of the strain, which can be expressed as

$$\varepsilon = \frac{\Delta L}{L} \tag{9}$$

where ε is the strain, ΔL is the relative deformation of the sample, and L is the original length of the sample. During the recover process, the sample was reheated. As the temperature increases, the sample recovered to the programmed shapes S2′, S1′ and S0′ at corresponding temperatures 55 °C, 85 °C and 130 °C. The recovered shapes S2′, S1′ and S0′ are in agreement with the programmed shapes S2, S1 and S0. This indicates that the sample exhibits multiple shape memory effect. Quantitative analysis of the shape recovery was also performed in the following sections.

Table 1. Parameters of the multiple shape memory model.

Model parameter	Value
Density of the polymer, ρ_n	874 kg m^{-3}
Gas constant, R	8.31 J mol^{-1} · K
Molecular weight, Mc	3.07×10^5 g mol^{-1}
Equilibrium Young's modulus, Y^{eq}	200 MPa
Nonequilibrium Young's modulus, Y_i^{neg}	1.19 kPa
Shape memory coefficient, a	1.32

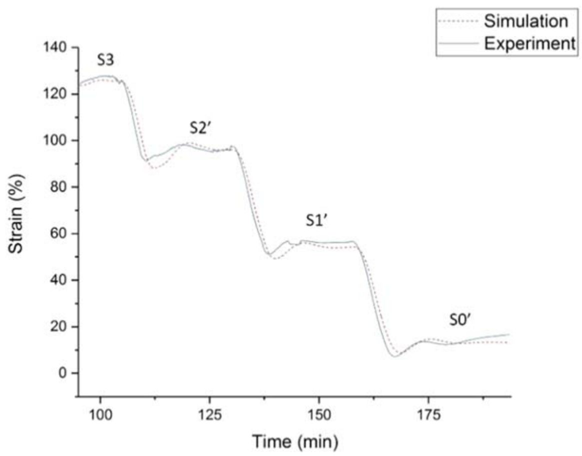

Figure 3. Comparison between simulation and experimental results for the multiple shape memory effect [31].

The model presented in section 2 was simulated using MATLAB. Table 1 shows the parameters of the multiple shape memory model. The nonequilibrium Young's modulus, molecular weight, and shape memory coefficient were fitted with the least-squares method. Figure 3 shows the comparison between the simulation and experimental results of the multiple shape memory effect where the simulated model is in good agreement with the experimental results. This suggests that the proposed model of memorized internal stresses can adequately represent the multiple shape effect of the MSM-IPMC.

3.2. Validation of the MSM-IPMC model

To validate the MSM-IPMC model in equation (6), the MSM-IPMC samples were tested. Three MSM-IPMC samples with

Table 2. Equivalent weight of Nafion, Aquivion, and GEFC membranes.

Membrane	Manufacturer	Structure	Equivalent weight (g/eq)
Nafion	DuPont	Perfluorovinyl ether groups terminated with sulfonate groups onto a tetrafluoroethylene backbone	1100
Aquivion	Solvay	Short Side Chain (SSC) copolymer of Tetrafluoroethylene (TFE) and Sulfonyl Fluoride Vinyl Ether (SFVE)	840
GEFC	GEFC	Perfluorinated backbone and sulfonate side chains	1000

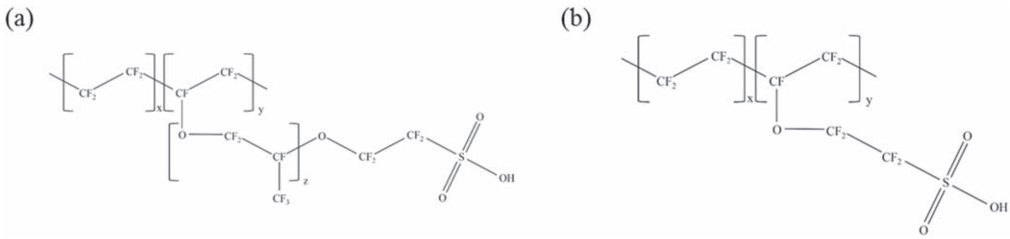

Figure 4. Polymer structures of different membranes [31]: (a) Nafion and GEFC, and (b) Aquivion.

Table 3. Dimensions of the MSM-IPMC membrane samples.

Item	W (mm)	L (mm)	$2h$ (mm)
Nafion	10.39	34.87	0.18
Aquivion	10.01	41.15	0.18
GEFC	9.92	36.12	0.29

different ionomer membranes, Nafion, Aquivion, and GEFC, were used. The properties of the membranes are presented in table 2 [34, 35]. Nafion contains perfluorovinyl ether groups terminated with sulfonate groups onto a tetrafluoroethylene backbone. As per the manufacturer Solvay, Aquivion is based on the Short Side Chain (SSC) copolymer of Tetrafluoroethylene (TFE) and Sulfonyl Fluoride Vinyl Ether (SFVE). The GEFC membrane has a perfluorinated backbone and sulfonate side chains similar to Nafion [35, 36]. The polymer structures of the membranes are shown in figure 4. It can be noticed that Aquivion has a shorter side chain compared with Nafion and GEFC. The sizes of the MSM-IPMC samples were measured and are shown in table 3.

Before the test, the samples were all programmed to several shapes. The original shape of the sample is identified as S0. The first shape S1 is memorized by folding the strip lengthwise around a rod, which was programmed at 85 °C and fixed at 70 °C. The second shape S2 is memorized by folding the strip lengthwise around the rod in the opposite direction, where the programming temperature is 55 °C and the fixing temperature is 22 °C. Figure 5 shows the experimental setup for the shape recovery process. A signal generator (SDG1025, Siglent) is used to provide the input signal for the electromechanical effect, which is amplified by a power amplifier (LVC-608, AE Techron, Inc.). Through the clamp contacts, a voltage input of 2 V amplitude and 1 Hz frequency is applied to the sample. The water is heated from room temperature (22 °C) to 90 °C using an immersion heater (3656K169, McMaster-Carr). To measure the water temperature, a circuit is developed based on a thermal resistor (PRTF-11-2-100-1/8-6-E, Omega®). A laser sensor (optoNCDT-1401, Micro-Epsilon) is used to measure the displacement of the sample. The voltage, current, displacement and temperature were measured simultaneously through the DAQ (NI SCB-68, National Instruments) and were recorded using the LabVIEW 8 Software.

Figure 6 shows the experimental results of the GEFC sample. It is observed that as the temperature increases, the voltage decreases while the current increases. Based on the results, it can be concluded that the electrical impedance of the MSM-IPMC decreases as the temperature increases. This property can be potentially used for thermal feedback control. Similar results were also found in the authors' previous study [25]. According to the displacement result, the sample shows the multiple shape memory effect and the electrical actuation effect simultaneously. The overall slow bending response of the sample resulted from the multiple shape memory effect. Increasing the temperature results in the sample recovering from S2 to S1′, where the sample visibly bends toward one side. As the temperature continues to increase, the sample then recovers to its original shape S0′, where the sample bends toward the other side. Meanwhile, the sample has an oscillation motion induced by the electromechanical actuation. It can be noted in the displacement curve in figure 6 that the peak to peak displacement increases with increasing temperature. This is possibly due to increased ion migration at higher temperatures, thermal expansion of the microchannels within the polymer itself, or a combination of effects. This is an area of further exploration.

Figure 7 shows the comparison between the experimental results and simulated results of the displacements of the MSM-IPMCs, which are based on Nafion, Aquivion, and GEFC membranes in Li^+-form. The results show that the model accurately describes the actual displacement of the different MSM-IPMCs. All three samples demonstrate the capability of the multiple shape memory effect. It was also

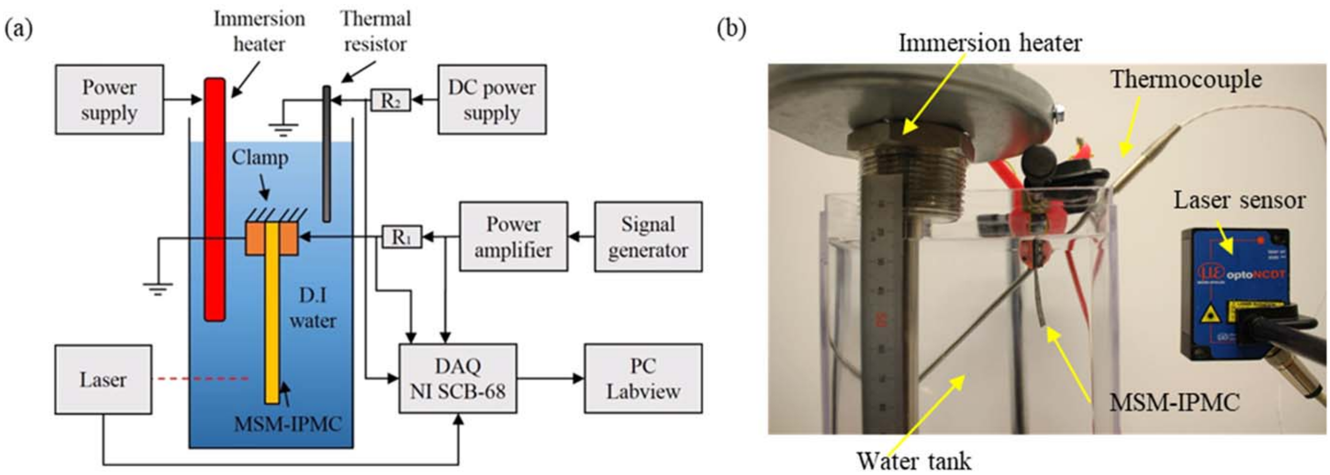

Figure 5. Experimental setup of the MSM-IPMC [31]: (a) Illustration, and (b) Photograph.

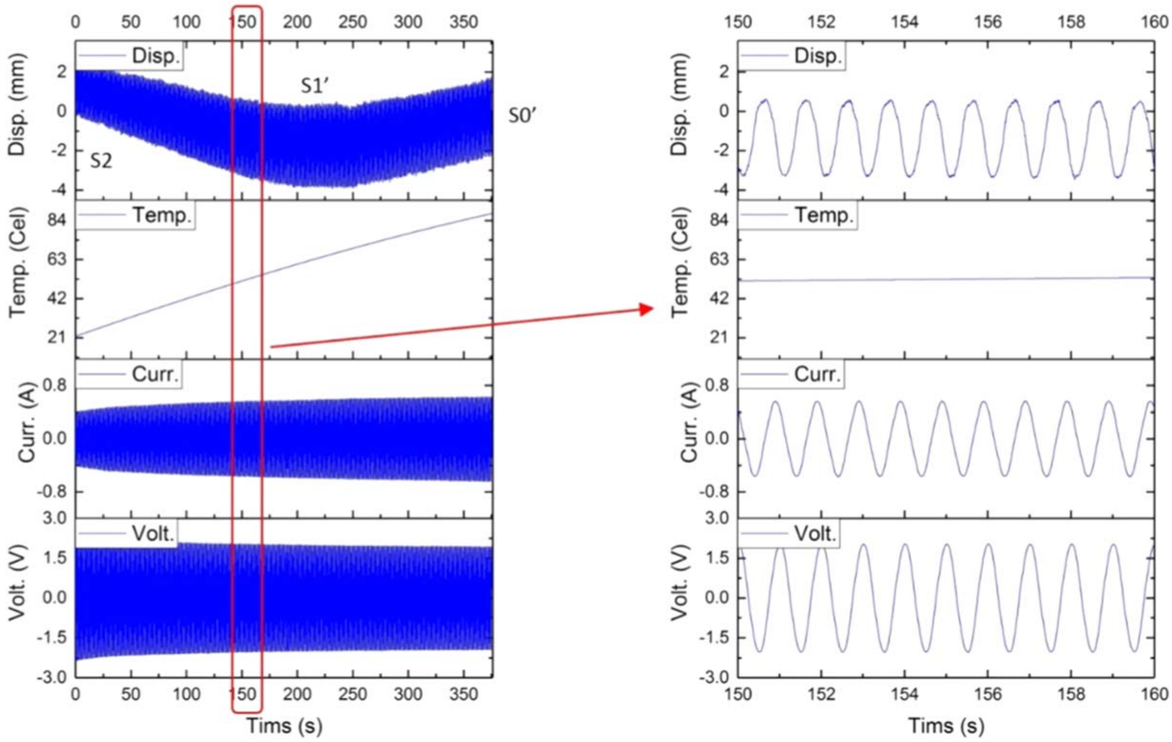

Figure 6. Measured displacement, temperature, current and voltage of GEFC sample. The full experiment is shown on the left with a magnified section shown on the right for better visualization [31].

found that the sample of Aquivion has the largest displacement, which is ~8 mm; the sample of Nafion and GEFC have relatively small displacements, which are ~2 mm and ~3 mm respectively. One contributing factor to the sample displacement differences is due to the longer length of the Aquivion versus both the Nafion and the GEFC samples. Another possible contribution is that Nafion and GEFC have a perfluorovinyl ether side group and a sulfonate end group. Aquivion has the sulfonyl fluoride vinyl ether as the side group, whose molecule chain is shorter. This short side chain enables the polymer to have a lower equivalent weight, which potentially causes a higher conductivity [34]. Furthermore, the Ion Exchange Capacity (IEC) of Aquivion is higher than the other two membranes, as shown in table 4. This also indicates the potential that Aquivion has better electromechanical performance than Nafion or GEFC.

3.3. Glass transition of different samples

The glass transitions of different membranes with different ions were studied. In this study, three different ionic exchange membranes were used, Nafion, Aquivion and GEFC. Each membrane has three different ion forms, Hydrogen (H^+), Lithium (Li^+) and Sodium (Na^+). Nine different samples in total were utilized for the test. By soaking the membranes in hydrogen chloride (HCl), Lithium chloride (LiCl) and Sodium chloride (NaCl) for the ionic exchange, the

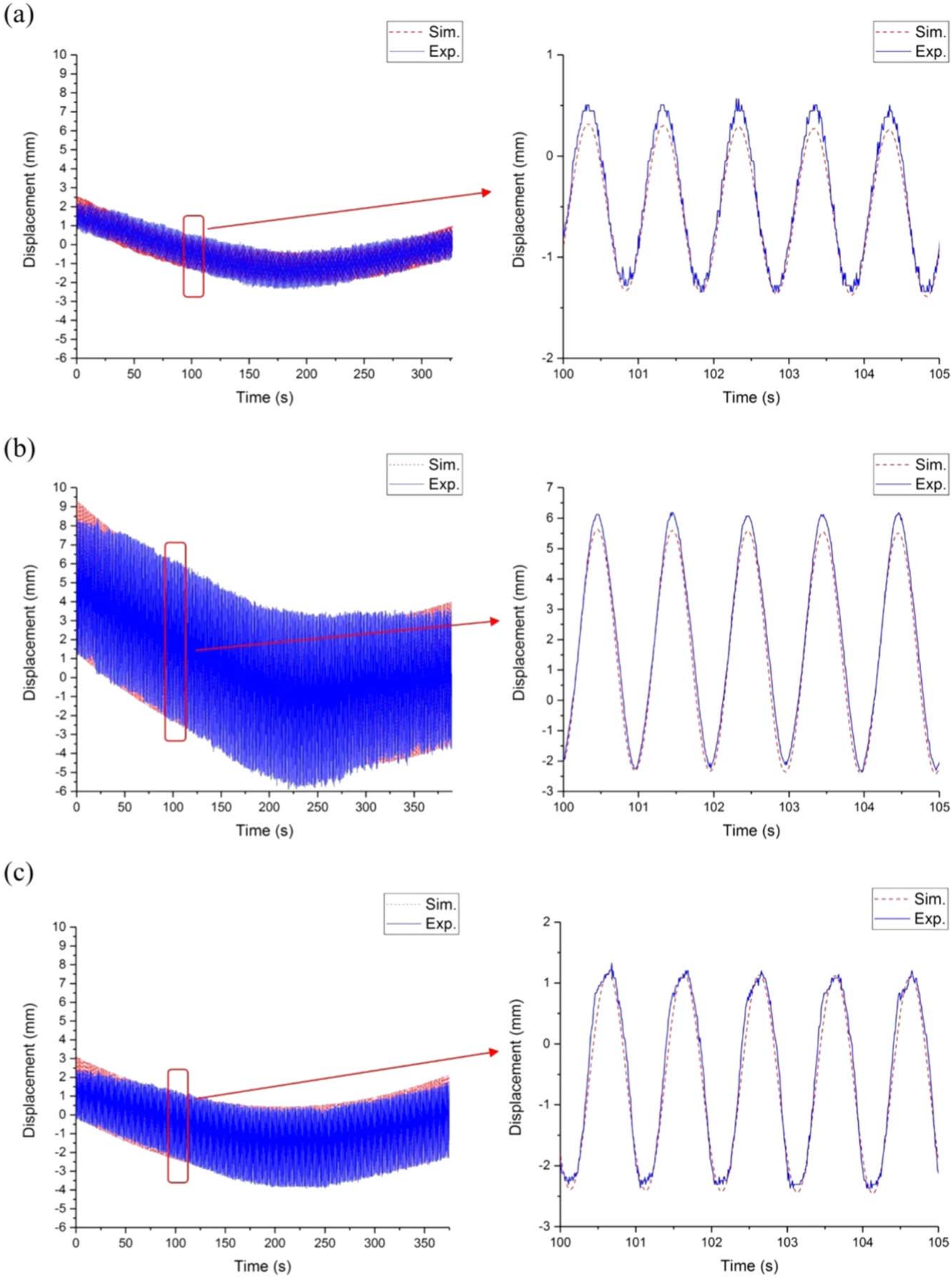

Figure 7. Comparison of theoretical and experimental results of different membrane based IPMCs [31]: (a) Nafion, (b) Aquivion, and (c) GEFC.

Table 4. Ion exchange capacity of each membrane material.

Membrane	Ion Exchange Capacity (meg/g)
Nafion	0.97 (±0.01) [Reference 35]
Aquivion	1.25 (±0.01) [Reference 34]
GEFC	0.95 (±0.01) [Reference 35]

membranes in H^+ form, Li^+ form and Na^+ form were obtained respectively. Prior to testing, the samples were annealed in an oven at 150 °C for 4 h to remove the residual stress/strain from the polymer processing step. The glass transition range of each sample is first measured separately. The mechanical properties of the samples were tested in DMA. The tangent of δ which is the ratio between the loss modulus E′ and the storage modulus E′, was then obtained. By measuring the start and end temperature of the tangent of δ curve peak, the broad glass transition can be derived [24].

Based on the experimental results, it was found that the membranes with the same ions have a similar glass transition range. Figure 8 shows an aggregation of the broad glass transition ranges for all membranes tested, sorted by ion type. The membranes in H^+-form have the shortest glass transition range, which is from ~50 °C to ~90 °C, the glass transition range of the membranes in Na^+-form is the longest, which is from ~55 °C to ~160 °C, and the Li^+-form membranes are between them, which is from ~55 °C to ~140 °C. It was also found that the H^+-form membranes have the lowest second glass transition temperature. The second glass transition temperature of the Na^+-form membrane is the highest. To explain this, the enthalpy and free energy of each ion were considered. This possible explanation is presented in the discussion section.

3.4. Shape recovery

The multiple shape memory effect was tested for each sample. Based on the obtained glass transition range of the different membranes (figure 8), the triple shape memory effect of the H^+-form MSM-IPMC, the quadruple shape memory effect of the Li^+-form MSM-IPMC, and the quintuple shape memory effect of the Na^+-form MSM-IPMCs were all tested. The number of shapes selected for each membrane type was based on the total number of shapes the authors were able to program within their given glass-transition region. Figure 9 shows the quintuple shape memory process of the Na^+-form MSM-IPMC. The results show that the sample has a recoverable multiple shape memory effect. To quantitatively analyze the multiple shape memory effect, the shape recovery rate of each sample during the shape memory process was calculated. Assuming the sample recovers from shape y to shape x, the shape recovery ratio $R_{f,x}$ of shape x can be calculated as

$$R_{f,x} = 100\% \times \frac{Sy - Sx'}{Sy - Sx} \quad (10)$$

where S_x, S_y are the strain at x and y during the shape programming process. $S_x{}'$ is the strain after recovery.

The shape recovery of the Na^+-form MSM-IPMCs was within the scope of 80% to 100%. The quintuple shape memory effect of the Na^+-form samples was demonstrated with the programming temperatures of ~45 °C, ~70 °C, ~95 °C and ~125 °C respectively.

3.5. Reversibility

In previous work, it was found that the multiple shape memory effect of the Nafion was reversible [24]. However, limited work was done regarding the reversibility of the membranes. The DMA was used to test the reversibility for an Aquivion sample containing Na^+ ions (figure 10). During the programming process, the sample with its original shape S0, was programmed at the temperature of 95 °C for shape S1 and 60 °C for shape S2. Then during the recovery process, the sample shows its reversibility between S0, S1 and S2 based on the temperature variation. The recovery sequence is from 1 to 9. It can be seen that the sample has good reversibility.

4. Discussion

4.1. Ionic effects on the membrane

The multiple shape memory effect of the ionic membranes used in this study likely results from the molecule chain motion of the membrane. From both the mathematical model proposed, and through experimental confirmation, this study analyzes two types of glass transition ranges. The first glass transition corresponds to the short-range segmental motions within a static electrostatic network where the multiple shape memory takes place. The second glass transition corresponds to the long-range molecular mobility due to the destabilization of the electrostatic network. The temperature range of the first and second glass transition regions are shown in figure 8. It was noticed that the H^+-form membranes have the lowest glass transition temperature, while the Na^+-form membranes have the highest. The glass transition temperature of the Li^+-form membranes is between the two other types but is closer to the latter. With a wider first glass transition region, the amount of possible programable shapes increases as shown with the quintuple shape memory effect of the Na^+-form MSM-IPMCs.

This can likely be attributed to the enthalpy and free energy of the different ions and can be explained as follows. When the membrane was heated, the enthalpy and the free energy of the membranes would be expected to increase. The enthalpy and free energy of the ions contribute to the total enthalpy and the free energy of the membrane. As the enthalpy and the free energy increase, the electrostatic network of the membrane starts to destabilize when the temperature is above the first glass transition range. Thus, the membranes with H + ions, whose enthalpy and free energy are the highest at around ~1500 kJ mol^{-1}, are the first to have the destabilized electrostatic network and have the lowest glass transition temperatures compared with the other two ionic form membranes [37]. The glass transition temperatures

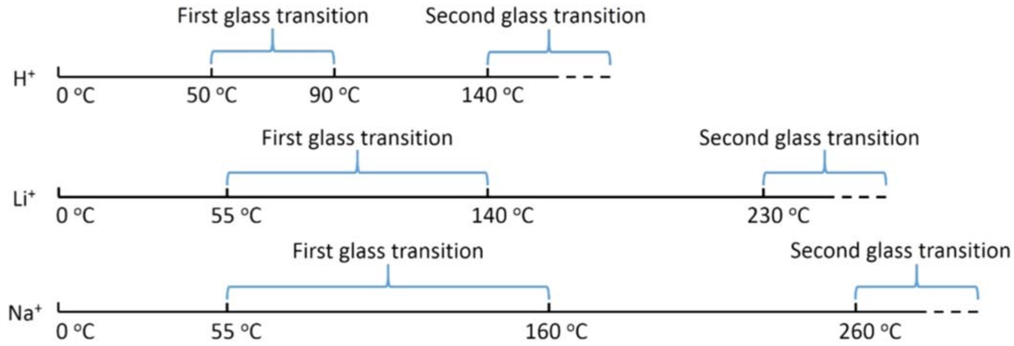

Figure 8. First and second glass transition ranges of membranes with different cations [31], H^+, Li^+, and Na^+.

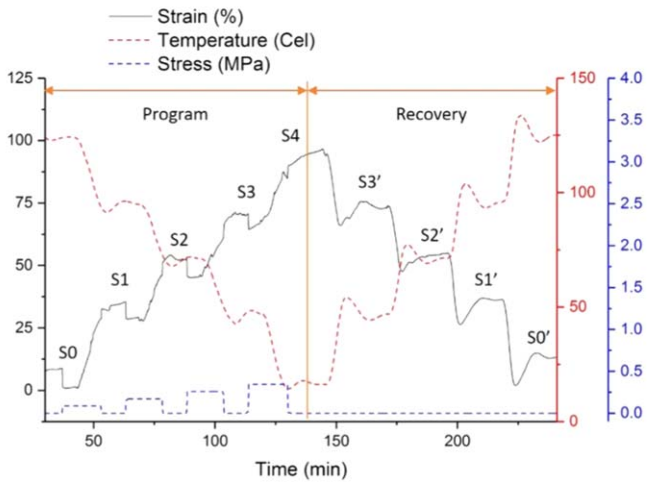

Figure 9. Quintuple shape memory process of the Na^+ form MSM-IPMC. In the left half of the plot, the programming stress and temperature ranges are shown for shapes S0 through S4. The right half of the plot shows the shape recovery [31].

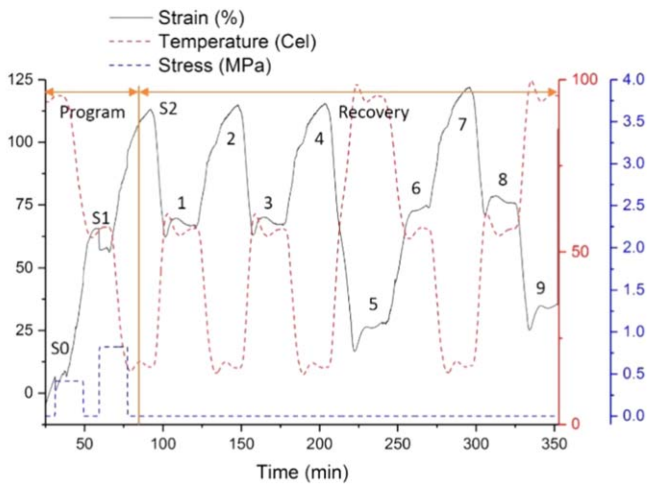

Figure 10. Multiple shape memory reversibility process of testing Na^+ form Aquivion. Two shapes S1 and S2 are programmed at temperatures 95 °C and 60 °C respectively. The temperature is then adjusted to cycle between shapes S1 and S2 before returning to shape S0 and subsequently followed by S1, S2, S1, and back to S0 [31].

of Li^+-form and Na^+-form membranes are higher, where the Na+-form membrane is relatively higher than the Li^+-form membrane. This has a good agreement with the enthalpy and free energy of Li^+ and Na^+ ions, where the Li^+ is relatively higher than the Na^+ at roughly ~685 kJ mol^{-1} and ~500 kJ/mol respectively [37]. This may offer an explanation to why the shape recovery of H^+-form membrane is lower than the other two membranes.

5. Conclusions

In this study, the MSM-IPMC was theoretically modeled and experimentally investigated. A theoretical model was proposed to describe the multiple shape memory effect of the MSM-IPMC, which was then coupled with an IPMC electromechanical model to obtain a complete physics-based model. The model was then validated through experimental analysis where the MSM-IPMC was able to successfully demonstrate the expected multiple shape memory properties. By comparing the simulation results of the model and the experimental results, it is found that the proposed model accurately describes the shape memory and electromechanical effects of an MSM-IPMC. The work in this paper is valuable for understanding the physical principles of the multiple shape memory effect.

The multiple shape memory effect was tested for three membrane types (Nafion, Aquivion, and GEFC) with varying ion forms. The experimental testing of glass transition temperature, shape recovery and reversibility were presented. All the samples were able to demonstrate the multiple shape memory effect with a differing number of capable programable shapes. This number was based on the obtained glass transition range for each respective ion type. It was found that the membranes with the H^+ ions have the lowest glass transition temperature and shape recovery, followed by membranes containing Li^+ ions, while membranes containing Na^+ ions had the highest of the two properties. A theory based on the enthalpy and free energy is proposed to explain this phenomenon. Furthermore, the shape recovery can be used to study the distribution of the quickly cycled transition temperatures of the membranes. The method is also valuable for the study of other shape memory polymers.

With the electromechanical and thermomechanical actuation, the MSM-IPMC actuator is capable of deformability and maneuverability of multiple degrees of freedom—the complex twisting, bending, and oscillating motions—with thermal and electrical control simultaneously or separately. This work is beneficial to future developments in soft-robotics and biomimetic studies.

Acknowledgments

Authors (Q S, N M, and K J K) acknowledge partial financial support from the US National Science Foundation (NSF), Partnerships for International Research and Education (PIRE) Program, Grant No. 1545857. Any opinions, findings, and conclusions or recommendations expressed in this material are those of the author(s) and do not necessarily reflect the views of the NSF. Also, this work was, in part, supported by the Department of Energy Minority Serving Institution Partnership Program (MSIPP) managed by the Savannah River National Laboratory under SRNS contract TOA#0000332975, for instrumentation. TS, NM and KJK acknowledge the partial financial support from the Office of Naval Research (N00014-16-1-2356) for fabrication of IPMC samples. IKO acknowledges the partial financial support from Creative Research Initiative Program (2015R1A3A2028975) funded by the National Research Foundation of Korea (NRF). Authors also thank Dr Taeseon Hwang of the University of Nevada, Las Vegas for assistance during the experimental investigation.

ORCID iDs

Kwang J Kim https://orcid.org/0000-0003-2134-4964

References

[1] Nam J, Hwang T, Kim K J and Lee D 2017 A new high-performance ionic polymer–metal composite based on Nafion/polyimide blends *Smart Mater. Struct.* **26** 35015
[2] Zhu Z, Wang Y, Liu Y, Asaka K, Sun X, Chang L and Lu P 2016 Application-oriented simplification of actuation mechanism and physical model for ionic polymer-metal composites *J. Appl. Phys.* **120** 34901
[3] He Q, Yu M, Yang X, Kim K J and Dai Z 2015 An ionic electro-active actuator made with graphene film electrode, chitosan and ionic liquid *Smart Mater. Struct.* **24** 65026
[4] Drozdov A D 2016 Modeling the response of polymer–ionic liquid electromechanical actuators *Acta Mech.* **227** 437
[5] Shen Q, Wang T, Wen L and Liang J 2013 Modelling and fuzzy control of an efficient swimming ionic polymer-metal composite actuated robot *Int. J. Adv. Robot. Syst.* **10** 1
[6] Kim K J, Palmre V, Stalbaum T, Hwang T, Shen Q and Trabia S 2016 Promising developments in marine applications with artificial muscles: electrodeless artificial cilia microfibers *Mar. Technol. Soc. J.* **50** 24
[7] Shen Q, Wang T and Kim K J 2015 A biomimetic underwater vehicle actuated by waves with ionic polymer–metal composite soft sensors *Bioinspir. Biomim.* **10** 55007
[8] Wang T, Shen Q, Wen L and Liang J 2012 On the thrust performance of an ionic polymer-metal composite actuated robotic fish: Modeling and experimental investigation *Sci. China Technol. Sci.* **55** 3359
[9] Shen Q, Kim K J and Wang T 2014 Electrode of ionic polymer-metal composite sensors: modeling and experimental investigation *J. Appl. Phys.* **115** 194902
[10] Wang Y, Chen H, Wang Y, Zhu Z and Li D 2014 Effect of Dehydration on the Mechanical and Physicochemical Properties of Gold- and Palladium -Ionomeric Polymer-Metal Composite (IPMC) Actuators *Electrochim. Acta* **129** 450
[11] Zhao D, Li D, Wang Y and Chen H 2016 Improved manufacturing technology for producing porous Nafion for high-performance ionic polymer–metal composite actuators *Smart Mater. Struct.* **25** 75043
[12] Wang Y, Zhu Z, Liu J, Chang L and Chen H 2016 Effects of surface roughening of Nafion 117 on the mechanical and physicochemical properties of ionic polymer–metal composite (IPMC) actuators *Smart Mater. Struct.* **25** 85012
[13] Shen Q, Palmre V, Stalbaum T and Kim K J 2015 A comprehensive physics-based model encompassing variable surface resistance and underlying physics of ionic polymer-metal composite actuators *J. Appl. Phys.* **118** 124904
[14] Cha Y and Porfiri M 2013 Bias-dependent model of the electrical impedance of ionic polymer-metal composites *Phys. Rev.* E **87** 22403
[15] Aureli M, Kopman V and Porfiri M 2010 Control-oriented modeling of ionic polymer metal composites for biomimetic underwater propulsion *American Control Conf. (ACC), 2010* p 6016
[16] Chen Z and Tan X 2008 A control-oriented and physics-based model for ionic polymer—metal composite actuators *IEEE/ASME Trans. Mechatronics* **13** 519
[17] Nemat-Nasser S 2002 Micromechanics of actuation of ionic polymer-metal composites *J. Appl. Phys.* **92** 2899
[18] Shen Q, Wang T, Liang J and Wen L 2013 Hydrodynamic performance of a biomimetic robotic swimmer actuated by ionic polymer–metal composite *Smart Mater. Struct.* **22** 75035
[19] Chae W, Cha Y, Peterson S D and Porfiri M 2015 Flow measurement and thrust estimation of a vibrating ionic polymer metal composite *Smart Mater. Struct.* **24** 95018
[20] Lei H, Sharif M A and Tan X 2016 Dynamics of omnidirectional IPMC sensor: experimental characterization and physical modeling *IEEE/ASME Trans. Mechatronics* **21** 601
[21] Abdulsadda A T and Tan X 2013 Underwater tracking of a moving dipole source using an artificial lateral line: algorithm and experimental validation with ionic polymer–metal composite flow sensors *Smart Mater. Struct.* **22** 45010
[22] Chen Z, Shatara S and Tan X 2010 Modeling of biomimetic robotic fish propelled by an ionic polymermetal composite caudal fin *IEEE/ASME Trans. Mechatronics* **15** 448
[23] Aureli M, Member S, Kopman V, Member S and Porfiri M 2010 Free-locomotion of underwater vehicles actuated by ionic polymer metal composites *IEEE/ASME Trans. Mechatronics* **15** 603
[24] Xie T 2010 Tunable polymer multi-shape memory effect *Nature* **464** 267
[25] Shen Q, Trabia S, Stalbaum T, Palmre V, Kim K and Oh I 2016 A multiple-shape memory polymer-metal composite actuator capable of programmable control, creating complex 3D motion of bending, twisting, and oscillation *Sci. Rep.* **6** 24462
[26] Rossiter J, Takashima K and Mukai T 2012 Shape memory properties of ionic polymer—metal composites *Smart Mater. Struct.* **21** 112002

[27] Xiao R, Guo J and Nguyen T D 2015 Modeling the multiple shape memory effect and temperature memory effect in amorphous polymers *RSC Adv.* **5** 416
[28] Zhao Q, Qi H J and Xie T 2014 Recent progress in shape memory polymer: new behavior, enabling materials, and mechanistic understanding *Prog. Polym. Sci.* **49** 79
[29] Shen Q, Palmre V, Kim K J and Oh I-K 2017 Theoretical and experimental investigation of the shape memory properties of an ionic polymer—metal composite *Smart Mater. Struct.* **26** 45020
[30] Shen Q, Palmre V, Stalbaum T and Kim K J 2015 Comprehensive modeling of ionic polymer-metal composite actuators based upon variable surface resistance and underlying physics of the polymer membrane *Proc. SPIE* **9432** 94302J
[31] Shen Q 2017 Theoretical and experimental investigation on the multiple shape memory ionic polymer-metal composite actuator *PhD Dissertation* University of Nevada, Las Vegas
[32] Tanaka F 2011 *Polymer Physics: Applications to Molecular Association and Thermoreversible Gelation* (Cambridge: Cambridge University Press)
[33] Nemat-Nasser S and Li J Y 2000 Electromechanical response of ionic polymer-metal composites *J. Appl. Phys.* **87** 3321
[34] Trabia S, Olsen Z and Kim K J 2017 Searching for a new ionomer for 3D printable ionic polymer-metal composites: Aquivion®as a candidate *Smart Mater. Struct.* **26** 115029
[35] Park J, Palmre V, Hwang T, Kim K, Yim W and Bae C 2014 Electromechanical performance and other characteristics of IPMCs fabricated with various commercially available ion exchange membranes *Smart Mater. Struct.* **23** 74001
[36] Palmre V, Pugal D, Kim K J, Leang K K, Asaka K and Aabloo A 2014 Nanothorn electrodes for ionic polymer-metal composite artificial muscles *Sci. Rep.* **4** 6176
[37] Ciferri A and Perico A 2012 *Ionic Interactions in Natural and Synthetic Macromolecules* (New York: Wiley)